OPAL PN300

July 25, 1997

Search for pair-produced scalar leptoquarks in e^+e^- interactions at $\sqrt{s} = 161$ and 172 GeV

OPAL Collaboration

Abstract

The results of a search for scalar leptoquarks of the first two generations at LEP2 energies are presented. The analysis has been performed using data samples of 9.9 pb^{-1} at an e^+e^- centre-of-mass energy $\sqrt{s} = 161$ GeV and 10.3 pb^{-1} at $\sqrt{s} = 172$ GeV, collected by the OPAL detector in 1996. The leptoquarks are assumed to be produced in pairs via gauge couplings to the photon and the Z^0. Summing over all possible decay channels, five candidate events are found, with an expectation of 7.6 events from Standard Model processes. Lower limits on leptoquark masses are improved in the region of large decay branching ratio to quark-ν.

This note describes preliminary OPAL results to be submitted to the XVIII International Symposium on Lepton-Photon Interactions, Hamburg, 28 July-1 August 1997, and to the International Europhysics Conference on High Energy Physics, Jerusalem, 19-26 August 1997.

1 Introduction

Quark and lepton degrees of freedom are very similar with respect to the family and multiplet structure of electroweak interactions. However, there is no justification, in the Standard Model, for such a symmetry. Some theories beyond the Standard Model (GUTs, compositeness and others [1]) predict the existence of new bosonic fields, called leptoquarks, carrying both lepton and baryon numbers. These particles could be pair produced, at LEP, by means of s-channel e^+e^- annihilation into γ or Z^0 as well as by t-channel exchange of a quark. Single leptoquark production should also be possible [2] via the process eq $\rightarrow$ leptoquark, where the quark originates from a hadronic fluctuation of a quasi-real photon radiated by one of the LEP beams. The interactions of leptoquarks with the known particles can be described by an effective Lagrangian respecting the $SU(3)_C \otimes SU(2)_L \otimes U(1)_Y$ symmetry of the Standard Model. With this assumption, the only free parameters are the leptoquark couplings to left- and right-handed fermions, $\lambda_{L,R}$, while the couplings to the electroweak gauge bosons are completely determined by the electric charge and the third component of the weak isospin. This results [3] in nine scalar leptoquarks (grouped into one weak isospin triplet, two doublets and two singlets) which conserve lepton as well as baryon number. In the present note, "state" will be used to refer to a charge eigenstate within a multiplet.

Several experimental results constrain the existence of leptoquarks. Low energy results favour those leptoquarks which couple diagonally, i.e. within a single fermion generation. LEP1 experiments [4] have excluded all types of leptoquarks with masses below about 45 GeV. The ZEUS [5] and H1 [6] experiments at HERA have searched for first generation leptoquarks. The results were obtained under the assumption that the members of the leptoquark multiplets are degenerate in mass. Leptoquark masses below about 80 GeV are excluded for λ values greater than a few 10^{-2} (about one order of magnitude smaller than the electromagnetic coupling $\lambda_e = 0.3$). The CDF [7] and D0 [8] experiments at the Fermilab Tevatron $p\bar{p}$ collider searched for first, second and third generation leptoquarks. In all the analyses performed, the channel where both leptoquarks decay into a quark and a neutrino was not searched for directly because of large background contributions. The two collaborations have placed limits on $\sigma_{\rm prod}\beta^2$ and $2\sigma_{\rm prod}\beta\,(1-\beta)$ as a function of the leptoquark mass; β is the decay branching ratio to quark-charged lepton. For low β values, the best limit is still the one given by the direct searches at LEP1. The search for pair production in e^+e^- or $p\bar{p}$ has the advantage that the production cross section is independent of the coupling λ. This is not the case for bounds from low energy experiments or from ep collisions at HERA.

This note describes a search for scalar leptoquarks of the first and second generation performed with the OPAL detector. The study is based on the data recorded during the 1996 LEP runs at centre-of-mass energies $\sqrt{s} = 161$ and 172 GeV, corresponding to integrated luminosities of 9.9 pb^{-1} and 10.3 pb^{-1}, respectively. In contrast to the analysis mentioned above, in this study limits are derived under the assumption that different states within leptoquark multiplets are not mass degenerate, but have different masses so that only one of the states contributes to the cross section at a time, because in the mass degenerated case the existing limits can not be improved. The branching ratio β of each state depends on the relative values of the leptoquark couplings to left- and right-handed fermions. Of the nine possible scalar states, six have $\beta \geq 0.5$: these states are therefore already excluded by CDF and D0 in the mass region accessible at LEP2 energies. The search was limited to the other three states; two of them,

$S_1(2/3)$ [1], and $\tilde{S}_{1/2}(1/3)$ have $\beta = 0$. The other state, $S_{1/2}(-2/3)$, has β ranging from 0 to 1. Only the pair production mechanism via s-channel e^+e^- annihilation was considered because the t-channel pair production, possible for first generation leptoquarks, contributes negligibly to the cross section for low values of λ.

2 The OPAL Detector and the Event Simulation

The OPAL detector, described in detail in [9], is a multipurpose apparatus with nearly complete solid angle coverage [2]. The central detector consists of a silicon microvertex detector and a system of tracking chambers inside a 0.435 T magnetic field. A lead-glass electromagnetic calorimeter together with presamplers and time-of-flight scintillators are located outside the magnet coil and in both endcaps. The magnet return yoke is instrumented for hadron calorimetry and is surrounded by external muon chambers. The forward detectors and silicon tungsten calorimeters, located on both sides of the interaction point, measure the luminosity and complete the geometrical acceptance down to 32 mrad in polar angle.

The decay of a large mass leptoquark into a quark and a charged lepton leads to final states characterized by an isolated energetic charged lepton, while for decays into a quark and a neutrino, the final state will have large missing energy. Three topologies are then possible for events that result from the decay of a leptoquark-antileptoquark pair:
(a) two hadronic jets and missing energy;
(b) two hadronic jets, one isolated charged lepton and missing energy;
(c) two hadronic jets and two isolated and oppositely charged leptons.
In all cases, the signal events are characterized by large charged multiplicities and large energy depositions, due to the hadronization of the $q\bar{q}$ pair.

The Monte Carlo generator LQ2 [10] was used to simulate leptoquark pair events. Initial state radiation was included and the hadronization of the $q\bar{q}$ pair was performed by the JETSET program, version 7.4. Both leptoquarks were forced to decay before hadronization started. The possibility that the couplings to fermions are small enough to let the two leptoquarks start fragmentation before they decay is taken into account introducing a systematic error in the signal efficiency. Samples of about 1000 signal events were generated, in steps of 5 GeV in the leptoquark mass, in the ranges 50 to 75 GeV (at $\sqrt{s} = 161$ GeV) and 55 to 80 GeV (at $\sqrt{s} = 172$ GeV), for the different decay topologies (a), (b) and (c) and for both first and second flavour generations. The full simulation of the OPAL detector [11] was then performed on generated events.
The sources of background from Standard Model processes to the leptoquark signal which were considered in the analysis at $\sqrt{s} = 161$ GeV are the following:

- Hadronic events from $e^+e^- \to Z^{0*}/\gamma^* \to q\bar{q}(\gamma)$.
  The PYTHIA [12] generator was used to simulate a sample of these events.

[1] In the notation adopted here, the index represents the weak isospin while the number in parenthesis is the electric charge. Thus, $S_1(2/3)$ is a member of a triplet of scalar states and its charge is Q = (2/3)e

[2] The coordinate system is defined so that z is the coordinate parallel to the e^+ and e^- beams, with positive direction along the e^- beam; r is the coordinate normal to the beam axis, ϕ is the azimuthal angle and θ is the polar angle with respect to $+z$.

- Four-fermion events.
  These events were simulated by EXCALIBUR [13], which takes into account all interfering diagrams and includes initial state radiation. However, EXCALIBUR does not simulate events in which one of the electrons scatters at a very small angle ($\leq$ 5°). Therefore, the following four-fermion processes were simulated separately:

- $e^+e^- \rightarrow We\nu$ and $e^+e^- \rightarrow (Z^{0*}/\gamma^*)e^+e^-$ events, generated with the PYTHIA and grc4f [14] Monte Carlos, respectively.

- Hadronic events from two-photon processes ($\gamma\gamma \rightarrow$ hadrons).
  The Monte Carlo generators PHOJET [15] and HERWIG [16] were used for generating two samples: the first contained events where the Q^2 of both photons is smaller than 1.0 GeV^2; the second contained higher Q^2 hadronic events.

- Four lepton $e^+e^-\tau^+\tau^-$ events.
  A Monte Carlo sample was produced with the generator of Vermaseren et al. [17]

Table 1 contains a summary of the background Monte Carlo samples at $\sqrt{s}$ = 161 GeV.
The background samples used in the analysis at $\sqrt{s}$ = 172 GeV were of the same kind except for four-fermion processes. These were simulated in separate samples, according to the flavour of the four-fermions and/or the diagrams leading to the final state, as shown in Table 2. The generators used were Vermaseren, grc4f and FERMISV [18]. Table 2 contains also all the other background samples at $\sqrt{s}$ = 172 GeV. As for signal events, all generated background samples were processed through the full simulation of the OPAL detector.

Background	Generator	$\int L(\mathrm{pb}^{-1})$
$Z^{0*}/\gamma^* \rightarrow q\bar{q}(\gamma)$	PYTHIA	339.2
4-fermion	EXCALIBUR	1168
$We\nu$	PYTHIA	13699
$(Z^{0*}/\gamma^*)\ e^+e^-$	grc4f	992.1
$\gamma\gamma \rightarrow$ hadrons ($Q^2 <$ 1. GeV^2)	PHOJET	69.8
$\gamma\gamma \rightarrow$ hadrons ($Q^2 >$ 1. GeV^2)	HERWIG	960.9
$e^+e^-\tau^+\tau^-$	Vermaseren	100.0

Table 1: Monte Carlo samples from Standard Model processes at $\sqrt{s}$ = 161 GeV.

Background	Generator	$\int L(\mathrm{pb}^{-1})$
$Z^{0*}/\gamma^* \to q\bar{q}(\gamma)$	PYTHIA	407.5
4 leptons (not $e^+e^-l^+l^-$)	grc4f	5000
2 leptons (not e^+e^-) qq	grc4f	5000
e^+e^- qq (s channel)	FERMISV	5000
qqqq	grc4f	5000
(Z^{0*}/γ^*) e^+e^-	grc4f	999.6
$\gamma\gamma \to$ hadrons ($Q^2 < 1.$ GeV^2)	PHOJET	50.3
$\gamma\gamma \to$ hadrons ($Q^2 > 1.$ GeV^2)	HERWIG	120.4
$e^+e^-\tau^+\tau^-$	Vermaseren+FERMISV	100+5000

Table 2: Monte Carlo samples from Standard Model processes at $\sqrt{s} = 172$ GeV.

3 Analysis

Charged tracks used in the calculation of physical variables were required to have at least 20 measured space points, at least 50% of the hits geometrically expected and a transverse momentum relative to the beam direction larger than 120 MeV. Good electromagnetic clusters are required to have an energy of at least 100 MeV in the barrel and 250 MeV in the endcaps. Endcap clusters were also required to contain at least two adjacent lead glass blocks. Clusters in the hadron calorimeter were required to have an energy larger than 0.6 GeV (2 GeV in the hadron poletips).
Calculations of experimental quantities like visible energy, transverse momentum, jets etc. were performed in the following way [19]. The four momenta of tracks and of electromagnetic and hadron calorimeter clusters not associated with charged tracks were first summed. When a calorimeter cluster had associated charged tracks, the expected calorimeter energy response for the associated charged track momenta was calculated and subtracted from the cluster energy to reduce double counting. If the energy of a cluster was smaller than the expected energy response of the associated tracks, the cluster energy was not used. The masses of all charged particles were set to the mass of the charged pion and the invariant masses of the energy clusters were assumed to be zero.

Events were preselected requiring that:

- the fraction of good charged tracks was greater than 0.2.
  This cut was intended to eliminate beam-wall and beam-gas interactions.

- the number of good charged tracks, n_{good}, was at least five and the number of good neutral electromagnetic clusters, $n^{EM}_{clusters}$, was at least five.

- the visible energy, E_{vis}, exceeded $0.2 \cdot \sqrt{s}$.
  The two last requirements discarded a large fraction of two-photon background events.

The selection procedures are different according to the following three classes of signal events:
Class A: two jets and two neutrinos;
Class B: two jets, one neutrino and one charged lepton of the first or second generation;
Class C: two jets and one pair of (oppositely) charged leptons of the first or second generation.

The selection of events of classes B and C requires charged lepton identification. Electron and muon identification was performed as described in ref. [20]. The energy of identified electrons was taken from the energy of the electromagnetic calorimeter cluster associated to the identified electron track, as resulted before the subtraction procedure described above. No attempt was made to identify the flavour of the quarks.

3.1 Class A

Signal events of class A are characterized by two acoplanar hadronic jets and missing energy. The following cuts were applied:

A1) the ratio $R_{vis} = E_{vis}/\sqrt{s}$ (where E_{vis} is the visible energy) had to fulfill the condition: $0.25 < R_{vis} < 0.75$;

A2) the cosine of the angle between the missing momentum and the z-axis, $\cos(\theta_{mis})$, was required to be: $|\cos(\theta_{mis})| < 0.9$;

A3) the missing transverse momentum $p_{t,mis}$ had to be greater than 15 GeV;

A4) the events were reconstructed into two jets using the Durham algorithm [21]: events with $y_{23} < 0.05$, where y_{23} is the resolution parameter at which the number of jets changes from two to three, were selected;

A5) the jets were required to be acoplanar by asking that $\cos(\phi_{jj}) > -0.95$ at $\sqrt{s} = 161$ GeV and $\cos(\phi_{jj}) > -0.85$ at $\sqrt{s} = 172$ GeV, where ϕ_{jj} is the angle between the projections of the jet directions onto the r-ϕ plane. The jets were also required to be acolinear by asking that $\cos(\theta_{jj}) > -0.85$ at $\sqrt{s} = 161$ GeV and $\cos(\theta_{jj}) > -0.65$ at $\sqrt{s} = 172$ GeV, where θ_{jj} is the angle between the two jet directions;

A6) the invariant mass of the two jets was required to lie outside the mass region between 75 GeV and 95 GeV;

A7) the events had to contain no identified charged leptons of energy greater than 15 GeV.

More stringent cuts on $\cos(\phi_{jj})$ and $\cos(\theta_{jj})$ were applied at $\sqrt{s} = 172$ GeV due to the higher background from W pairs. Selections from A1 to A3 are useful, in particular, in rejecting two-photon background. Cuts A2 and A5 reduce $Z^{0*}/\gamma^* \to q\bar{q}$ events, while A4, A6 and A7 are designed against four-fermion background. Three events in the data survive the selection at

	Data	**tot. bkg.**	4-fermions	$\gamma\gamma \to$ had.	$Z^{0*}/\gamma^* \to q\bar{q}$	**Eff. (%)**
Presel.	4847	4388.3	80.0	2910.2	1398.1	93.6
Cut (A1)	2677	2349.5	37.0	1672.1	640.4	88.5
Cut (A2)	201	175.2	12.2	122.2	40.8	78.0
Cut (A3)	34	23.7	9.4	0.3	14.0	71.6
Cut (A4)	27	18.6	5.5	0.3	12.8	68.9
Cut (A5)	6	2.9	2.8	0.	0.1	52.2
Cut (A6)	3	1.7	1.6	0.	0.1	45.1
Cut (A7)	3	1.2	1.1	0.	0.1	43.6

Table 3: The remaining numbers of events after each cut of selection A for various background processes normalised to 9.9 pb^{-1} are compared with data at $\sqrt{s} = 161$ GeV. The last column reports the signal efficiency, in percent, for events with $M_{LQ} = 65$ GeV.

$\sqrt{s} = 161$ GeV while no events are retained at 172 GeV. The number of expected background events from Standard Model processes is 1.2 at $\sqrt{s} = 161$ GeV and 1.1 at 172 GeV. Figure 1

	Data	**tot. bkg.**	4-fermions	$\gamma\gamma \rightarrow$ had.	$Z^{0*}/\gamma^* \rightarrow q\bar{q}$	**Eff. (%)**
Presel.	4904	4562.7	161.5	3193.8	1207.4	95.9
Cut (A1)	2697	2420.3	64.6	1783.9	571.8	90.3
Cut (A2)	191	176.9	33.6	112.7	30.6	81.1
Cut (A3)	56	41.3	29.6	0.4	11.3	74.5
Cut (A4)	36	25.9	15.1	0.4	10.4	71.6
Cut (A5)	1	3.2	3.2	0.	0.	51.4
Cut (A6)	1	2.1	2.1	0.	0.	43.0
Cut (A7)	0	1.1	1.1	0.	0.	41.6

Table 4: Same as Table 3, at $\sqrt{s} = 172$ GeV. The various background processes are normalised to an integrated luminosity of 10.3 pb^{-1}.

shows the distributions of two of the most powerful cut variables, at various stages of the selection procedure, for the data, the simulated background and the simulated signal with $M_{LQ} = 65$ GeV. Tables 3 and 4 contain the number of events after each cut, compared with the number of background events as predicted from Monte Carlo samples and with the efficiencies for signal events from the sample of $M_{LQ} = 65$ GeV. Other Standard Model processes like $e^+e^- \rightarrow Z^{0*}/\gamma^* \rightarrow \tau^+\tau^-(\gamma)$ have been checked to contribute negligibly to the background.

3.2 Class B

The selection of signal events of this class proceeded as follows:
B1) R_{vis} had to fulfill the condition $0.5 < R_{vis} < 1$;
B2) the cosine of the angle between the missing momentum and the z-axis, $\cos(\theta_{mis})$, was required to be: $\mid \cos(\theta_{mis}) \mid < 0.9$;
B3) the ratio R_{mis} between the absolute value of the missing momentum and $\sqrt{s}$ was required to satisfy: $R_{mis} > 0.08$;
B4) at least one identified charged lepton with minimal energy of 14 GeV was required;
B5) no charged tracks and at most one electromagnetic cluster had to lie inside a cone of half-aperture 20° around the most energetic lepton;
B6) after having removed the most energetic lepton, the event was forced to 2-jets. The jets were required to be acolinear: the angle θ_{jj} between the jet directions had to be $\cos(\theta_{jj}) > -0.85$ at $\sqrt{s} = 161$ GeV and $\cos(\theta_{jj}) > -0.65$ at $\sqrt{s} = 172$ GeV;
B7) the invariant mass of the two jets was required to lie outside the mass region between 75 GeV and 85 GeV.

Two-photon events contribute negligibly to the background after selection B4. Cuts B2, B4, B6 and B7 are particularly efficient in reducing four-fermion background, while cuts B2, B4 and B5 reduce $Z^{0*}/\gamma^* \rightarrow q\bar{q}$ events. In total, two events in the data are retained after the selection for the first generation, in agreement with an expected background of 1.7 events. For the second generation, 1.7 events are expected and none observed. A small fraction of simulated four-fermion events passed both selection A and selection B: this corresponds to about 4% of the total background estimated for selection B. Figure 2 shows the distributions of some cut variables at various stages of the selection procedure. The tables 5 and 6 contain the number of events after each cut, compared with the number of background events as predicted from Monte Carlo samples and with the efficiencies for signal events with $M_{LQ} = 65$ GeV.

	Data	**tot. bkg.**	4-fermions	$\gamma\gamma \to$ had.	$Z^{0*}/\gamma^* \to q\bar{q}$	**Eff. (%)**
Presel.	4847	4388.3	80.0	2910.2	1398.1	97.2/98.0
Cut (B1)	1560	1420.6	57.6	305.0	1058.0	94.4/88.8
Cut (B2)	346	336.2	28.5	4.3	303.4	83.3/80.3
Cut (B3)	177	142.2	18.6	1.0	122.6	80.0/79.6
Cut (B4)	42/16	30.4/13.9	5.8/5.2	0.1/0.	24.5/8.7	70.6/72.0
Cut (B5)	4/1	3.9/3.2	3.1/3.2	0.1/0.	0.7/0.	60.0/63.1
Cut (B6)	1/0	1.0/1.0	0.9/1.0	0./0.	0.1/0.	50.3/51.9
Cut (B7)	1/0	0.7/0.8	0.7/0.8	0./0.	0./0.	46.1/48.8

Table 5: The remaining numbers of events after each cut of selection B for various background processes normalised to 9.9 pb^{-1} are compared with data at $\sqrt{s}$ = 161 GeV. The last column reports the signal efficiency, in percent, for events with M_{LQ} = 65 GeV. When two numbers are separated by a slash, the first one refers to the first generation and the second one to the second generation.

	Data	**tot. bkg.**	4-fermions	$\gamma\gamma \to$ had.	$Z^{0*}/\gamma^* \to q\bar{q}$	**Eff. (%)**
Presel.	4904	4562.7	161.5	3193.8	1207.4	99.3/98.3
Cut (B1)	1521	1532.7	120.3	514.8	897.6	96.7/91.5
Cut (B2)	317	353.2	82.8	14.9	255.5	87.6/82.9
Cut (B3)	173	156.9	57.9	1.7	97.3	86.0/80.7
Cut (B4)	49/23	42.4/24.3	21.4/17.1	0.1/0.	20.9/7.2	75.6/73.4
Cut (B5)	11/8	12.5/11.1	11.9/11.1	0.1/0.	0.5/0.	65.0/66.0
Cut (B6)	1/0	1.4/1.3	1.4/1.3	0./0.	0./0.	43.5/44.2
Cut (B7)	1/0	1.0/0.9	1.0/0.9	0./0.	0./0.	40.5/40.8

Table 6: Same as Table 5 at $\sqrt{s}$ = 172 GeV. The various background processes are normalised to 10.3 pb^{-1}.

3.3 Class C

Signal events of this type have small missing energy and are characterized by the presence of a pair of high energy charged leptons that tend to be isolated. The following cuts were applied to select class C events:
C1) R_{vis} had to fulfill the condition $0.75 < R_{vis} < 1.25$;
C2) the events were reconstructed into four jets using the Durham algorithm: events with $y_{34} > 0.001$, where y_{34} is the resolution parameter at which the number of jets changes from four to three, were selected;
C3) at least one pair of identified oppositely charged leptons of the first or second generation;
C4) at $\sqrt{s}$ = 161 GeV the energy of the most energetic muon (electron) of the pair had to exceed 22 GeV (20 GeV), while a minimal energy of 15 GeV (12 GeV) was required for the other muon (electron). At $\sqrt{s}$ = 172 GeV the minimal energy of the most energetic muon (electron) of the pair was increased to 25 GeV (22 GeV);
C5) no charged tracks and at most one electromagnetic cluster had to lie inside a cone of half-aperture 15° around the most energetic lepton.

Background from two-photon events is largely removed after selection C3. Cuts C3 and C4 are efficient against both four-fermion and $Z^{0*}/\gamma^* \to q\bar{q}$ events. The lepton isolation requirement

	Data	**tot. bkg.**	4-fermions	$\gamma\gamma \to$ had.	$Z^{0*}/\gamma^* \to q\bar{q}$	**Eff. (%)**
Presel.	4847	4388.3	80.0	2910.2	1398.1	98.5/98.1
Cut (C1)	862	807.4	41.3	21.6	744.5	94.3/93.7
Cut (C2)	463	424.2	31.2	14.3	378.7	91.5/89.8
Cut (C3)	58/75	43.6/83.0	4.9/7.5	0.2/0.6	38.5/74.9	77.5/80.9
Cut (C4)	7/0	5.7/0.6	0.8/0.4	0./0.	4.9/0.2	73.8/76.6
Cut (C5)	0/0	0.6/0.2	0.5/0.2	0./0.	0.1/0.	72.7/73.6

Table 7: The remaining numbers of events after each cut of selection C for various background processes normalised to 9.9 pb^{-1} are compared with data at $\sqrt{s} = 161$ GeV. The last column reports the signal efficiency, in percent, for events with $M_{LQ} = 65$ GeV. When two numbers are separated by a slash, the first one refers to the first generation and the second one to the second generation.

	Data	**tot. bkg.**	4-fermions	$\gamma\gamma \to$ had.	$Z^{0*}/\gamma^* \to q\bar{q}$	**Eff. (%)**
Presel.	4904	4562.7	161.5	3193.8	1207.4	99.0/98.0
Cut (C1)	771	836.2	94.8	120.9	620.5	97.4/94.6
Cut (C2)	446	483.6	79.0	100.2	304.4	94.9/89.4
Cut (C3)	50/72	47.1/84.6	13.8/21.1	1.2/0.5	32.1/63.0	79.5/80.7
Cut (C4)	8/0	5.3/0.7	1.7/0.4	0./0.	3.6/0.3	74.5/73.8
Cut (C5)	0/0	0.9/0.2	0.8/0.2	0./0.	0.1/0.	72.2/67.4

Table 8: Same as Table 7, at $\sqrt{s} = 172$ GeV. The various background processes are normalised to 10.3 pb^{-1}.

C5 is also very efficient in reducing $Z^{0*}/\gamma^* \to q\bar{q}$ background. The selection eliminates all data events; 1.5 background events for the first generation and 0.4 for the second generation are expected. Figure 3 shows the distributions of the main cut variables at various stages of the selection procedure. Tables 7 and 8 contain the number of events after each cut, compared with the number of background events as predicted from Monte Carlo samples and with the efficiencies for signal events with $M_{LQ} = 65$ GeV.

4 Results

The efficiencies for signal events, as functions of the leptoquark mass M_{LQ}, are listed in tables 9 and 10. Production cross sections, as functions of M_{LQ}, have been computed: figure 4 shows

LQ mass (GeV)	50	55	60	65	70	75
Signal topology						
Class A	37.5	35.7	37.7	43.6	46.3	50.1
Class B (first gen.)	39.6	37.9	42.2	46.1	46.4	49.2
Class B (second gen.)	48.0	43.5	45.2	48.8	44.8	50.6
Class C (first gen.)	71.5	71.6	71.9	72.7	70.2	65.3
Class C (second gen.)	64.9	68.8	69.2	73.6	70.8	67.6

Table 9: The detection efficiencies in percent for selections at $\sqrt{s} = 161$ GeV.

LQ mass (GeV)	55	60	65	70	75	80
Signal topology						
Class A	29.5	34.3	41.6	43.1	46.1	49.5
Class B (first gen.)	32.5	36.3	40.5	38.6	40.3	43.7
Class B (second gen.)	36.3	37.6	40.8	46.5	46.7	49.8
Class C (first gen.)	66.7	70.8	72.2	66.0	68.1	64.8
Class C (second gen.)	61.1	64.3	67.4	67.0	67.9	68.0

Table 10: The detection efficiencies in percent for selections at $\sqrt{s}$ = 172 GeV.

the cross sections of the states $S_1(2/3)$, $\tilde{S}_{1/2}(1/3)$ and $S_{1/2}(-2/3)$ at $\sqrt{s}$ = 161 and 172 GeV. The t-channel contribution, possible for the first generation state $S_{1/2}(-2/3)$, was neglected. Within this assumption, production cross sections depend only on the (known) couplings of the leptoquarks to the electroweak gauge bosons.

For each leptoquark mass $\mathrm{M_{LQ}}$ and branching fraction β, the number of expected signal events is given by the following expression:

$$N_{\mathrm{expected}}^{\mathrm{signal}} = \sigma_{\mathrm{prod}}\ (M_{\mathrm{LQ}})\ \cdot\ \left[\epsilon_{\mathrm{C}}\beta^2 + \epsilon_{\mathrm{B}}\ 2\beta\ (1-\beta) + \epsilon_{\mathrm{A}}\ (1-\beta)^2\right]\ \cdot\ \int Ldt \qquad (1)$$

where σ_{prod} is the production cross section, ϵ_{A}, ϵ_{B} and ϵ_{C} are the efficiencies of the selection procedure for signal events of classes A, B and C, respectively; $\int Ldt$ is the integrated luminosity. The number of expected signal events has been computed by means of equation (1) as a function of the leptoquark mass: at $\sqrt{s}$ = 161 GeV in the range 50 GeV $\leq \mathrm{M_{LQ}} \leq$ 75 GeV and at $\sqrt{s}$ = 172 GeV in the range 55 GeV $\leq \mathrm{M_{LQ}} \leq$ 80 GeV.

The systematic effects arising from the following sources were evaluated:

- the errors due to signal Monte Carlo statistics and the interpolation errors at an arbitrary point of $\mathrm{M_{LQ}}$ were estimated to be 4–9%, depending on the signal topology;
- the error associated to the lepton identification method was 1.0% for the electron and 1.2% for the muon identification;
- the uncertainty introduced by the acolinearity and acoplanarity cuts in the selections of class A and B events was evaluated smearing the jet directions according to a gaussian probability distribution with rms deviation σ = 60 mrad, and found to contribute with a 3.0%;
- the systematic error associated to the fragmentation of the leptoquark decay products was estimated to be about 10%. This was evaluated comparing the signal efficiencies with the efficiencies obtained applying the same selection cuts to signal events in which the leptoquark couplings to fermions are assumed small enough to let the two leptoquarks start fragmentation before they decay;
- the error on the integrated luminosity was 0.7% either at $\sqrt{s}$ = 161 GeV or at $\sqrt{s}$ = 172 GeV.

The systematic error due to the trigger efficiency was negligible for the selected signal events. The errors were considered to be independent and added in quadrature.

4.1 Limits

No evidence of leptoquark production was observed in the data. Excluded regions in the β-$\mathrm{M_{LQ}}$ plane were determined, at the 95% C.L., using the procedure described in [22]. In calculating the limits, the systematic errors were treated as in [23]. The results obtained at the two energies were combined: the state $S_1(2/3)$ is excluded for masses below 73.4 GeV, as shown in figure 5 (a), and the state $\tilde{S}_{1/2}(1/3)$ for masses below 53.0 GeV, figure 5 (b) [3]. The excluded regions of the plane β-$\mathrm{M_{LQ}}$ for $S_{1/2}(-2/3)$ are reported in figures 6 (a) and 6 (b) for the first and second generation, respectively.

5 Conclusions

Two data samples collected with the OPAL detector at $\sqrt{s}$ = 161 GeV and at $\sqrt{s}$ = 172 GeV were analysed to search for scalar leptoquarks of the first and second generations. The used data correspond to integrated luminosities of 9.9 $\mathrm{pb^{-1}}$ and 10.3 $\mathrm{pb^{-1}}$, respectively. Five events in the data pass the selections, with an expectation of 7.6 events from Standard Model processes. Lower mass limits for scalar leptoquarks were set by combining the data at the two energies. The present analysis improves existing limits, under the assumption that the leptoquark multiplets are non degenerate in mass, for those states with possible values of β lower than 0.5.

[3]The limit on $\tilde{S}_{1/2}(1/3)$ is also valid for the third generation; the same is not true for the limit on $S_1(2/3)$, since the third generation state, under the hypothesis of diagonal coupling, decays to a top quark and a ν_τ

References

[1] J.C. Pati and A. Salam, Phys. Rev. D10 (1974) 275;
E. Farhi and L. Susskind, Phys. Rep. 74 (1981) 277;
L. Lyons, Progr. Part. Nucl. Phys. 10 (1982) 227;
B. Schrempp and F. Schrempp, Phys. Lett. B153 (1985) 101;
J.L. Hewett and T.G. Rizzo, Phys. Rep. 183 (1989) 193;
P.H. Frampton, Mod. Phys. Lett. A7 (1992) 559;
J.L. Hewett and T.G. Rizzo, SLAC-PUB-7430, March 1997.

[2] M. Doncheski and S. Godfrey, Phys. Lett. B393 (1997) 355;
OPAL Physics Note PN 288 (1997).

[3] J. Buchmüller, R. Rückl and D. Wyler, Phys. Lett. B191 (1987) 442;
J. Blümlein and R. Rückl, Phys. Lett. B304 (1993) 337;
J. Blümlein, E. Boos, Nucl. Phys. (Proc. Suppl.) B37 (1994) 181.

[4] OPAL Collab., G. Alexander *et al.*, Phys. Lett. B263 (1991) 123;
L3 Collab., B. Adeva *et al.*, Phys. Lett. B261 (1991) 169;
DELPHI Collab., P. Abreu *et al.*, Phys. Lett. B275 (1992) 222;
ALEPH Collab., D. DeCamp *et al.*, Phys. Rep. 216 (1992) 253.

[5] ZEUS Collab., M. Derrick *et al.*, Phys. Lett. B306 (1993) 173.

[6] H1 Collab., T. Ahmed *et al.*, Z. Phys. C64 (1994) 545;
H1 Collab., S. Aid *et al.*, Phys. Lett. B369 (1996) 173.

[7] CDF Collab., F. Abe *et al.*, Phys. Rev. D48 (1993) 3939;
CDF Collab., F. Abe *et al.*, Phys. Rev. Lett. 75 (1995) 1012.

[8] D0 Collab., S. Abachi *et al.*, Phys. Rev. Lett. 72 (1994) 965;
D0 Collab., S. Abachi *et al.*, Phys. Rev. Lett. 75 (1995) 3618.

[9] OPAL Collab., K. Ahmet *et al.*, Nucl. Instr. Meth. A305 (1991) 275;
P.P. Allport *et al.*, Nucl. Instr. Meth. A324 (1993) 34;
P.P. Allport *et al.*, Nucl. Instr. Meth. A346 (1994) 476;
B.E. Anderson *et al.*, IEEE Trans. on Nucl. Science 41 (1994) 845.

[10] D.M. Gingrich, in "Physics at LEP2" CERN Yellow Report, Vol. 2, Geneva (1996) 345.

[11] J. Allison *et al.*, Nucl. Instr. Meth. A317 (1992) 47.

[12] T. Sjöstrand, Comp. Phys. Comm. 39 (1986) 347;
T. Sjöstrand, PYTHIA 5.7 and JETSET7.4 Manual, CERN-TH 7112/93.

[13] F.A. Berends, R. Pittau, R. Kleiss, Comp. Phys. Comm. 85 (1995) 437.

[14] J. Fujimoto *et al.*, KEK-CP-046 (1996).

[15] R. Engel and J. Ranft, Phys. Rev. D54 (1996) 4244;
R. Engel, Z. Phys. C66 (1995) 203.

[16] G. Marchesini, B.R. Webber, G. Abbiendi, I.G. Knowles, M.H. Seymour and L. Stanco, Comp. Phys. Comm. 67 (1992) 203.

[17] J.A.M. Vermaseren, Nucl. Phys. B229 (1983) 347.

[18] J. Hilgart, R. Kleiss and F. LeDiberder, Comp. Phys. Comm. 75 (1993) 191.

[19] OPAL Collab., K. Ackerstaff *et al.*, Phys. Lett. B389 (1996) 616.

[20] OPAL Collab., K. Ackerstaff *et al.*, Phys. Lett. B389 (1996) 416.

[21] S. Catani *et al.*, Phys. Lett. B269 (1991) 432.

[22] Particle Data Group, Phys. Rev. D54 (1996) 1.

[23] R.D. Cousins and V.L. Highland, Nucl. Instr. Meth. A320 (1992) 331.

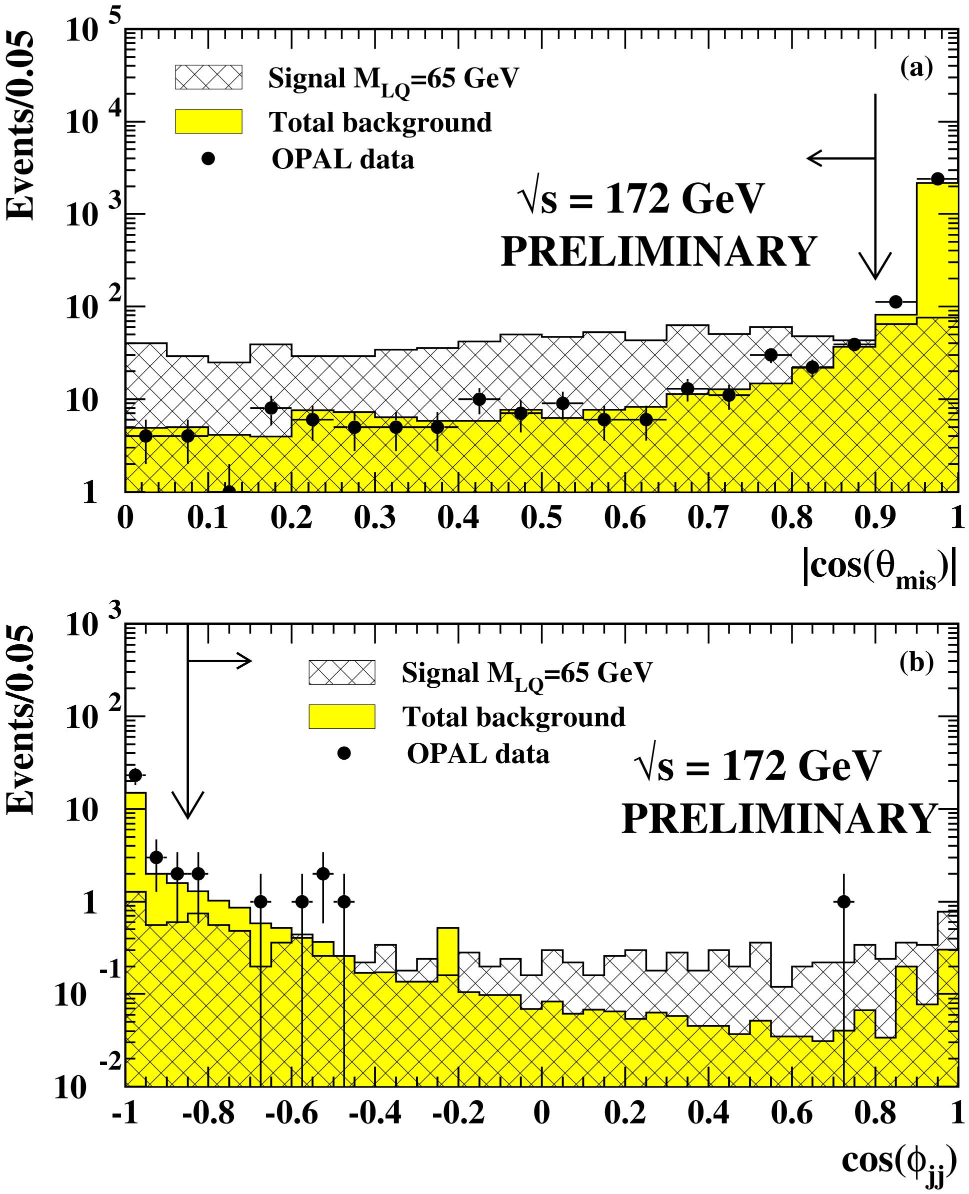

Figure 1:
(a) The number of events versus $|\cos(\theta_{\mathrm{mis}})|$ for the data at $\sqrt{s} = 172$ GeV after the preselection and cut A1. Also shown is the same distribution for the total simulated background and for simulated leptoquark signal events of class A with $M_{LQ} = 65$ GeV.
(b) The number of events versus the acoplanarity at $\sqrt{s} = 172$ GeV after the preselection and cuts A1-A5.

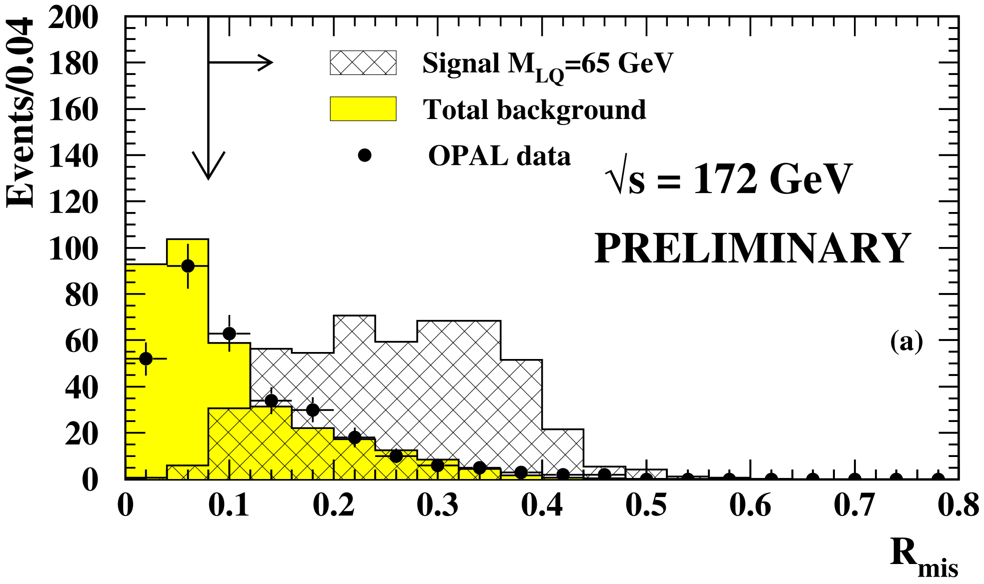

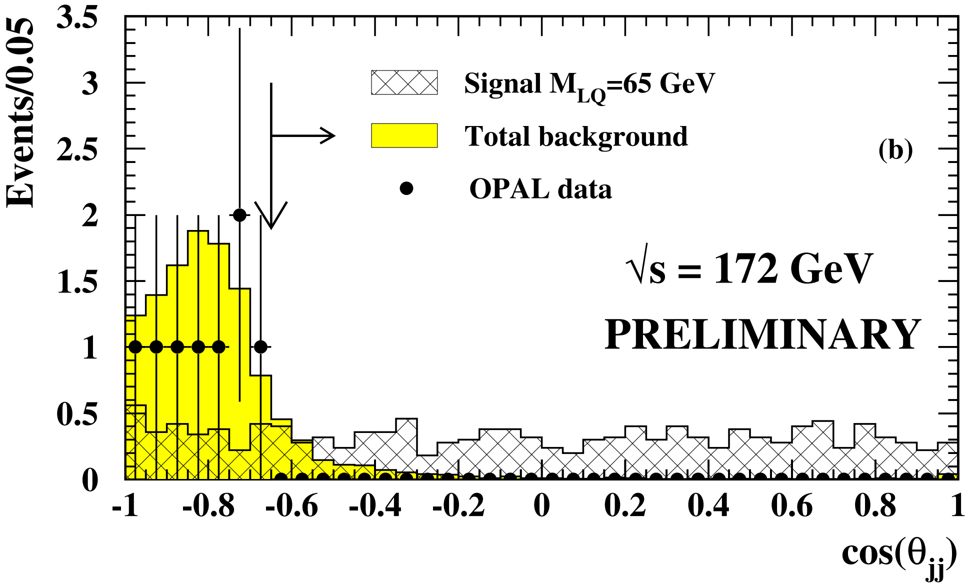

Figure 2:
(a) The number of events versus $R_{mis} = p_{mis}/\sqrt{s}$ at $\sqrt{s}$ = 172 GeV after the preselection and cuts B1-B2. The symbols are as defined in figure 1; signal events are of class B.
(b) The number of events versus the acolinearity of the two jets obtained after the removal of the most energetic muon (see the definition of selection B6 in the text) at $\sqrt{s}$ = 172 GeV. Preselection and cuts B1-B5 have been applied.

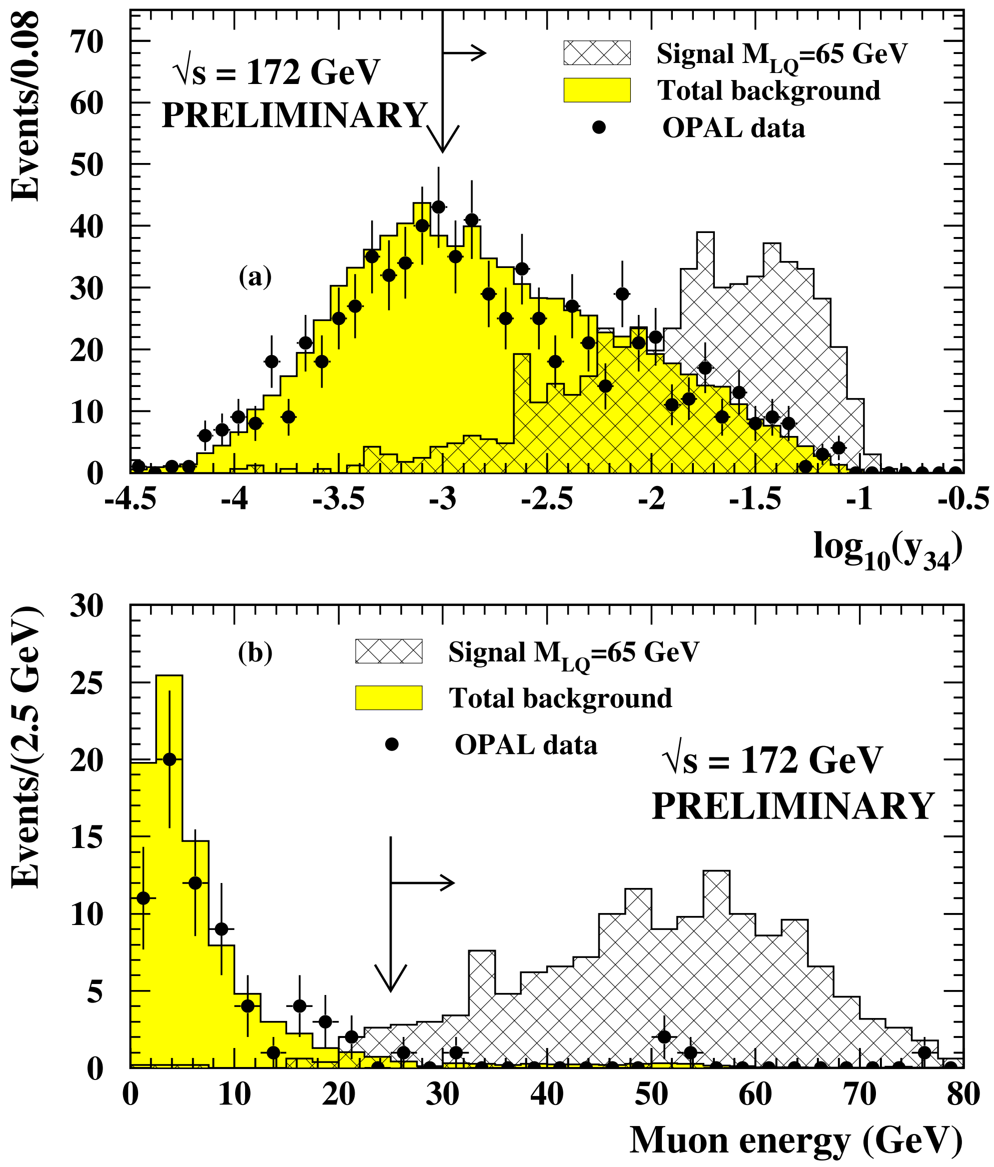

Figure 3:
(a) The number of events versus the logarithm of y_{34} at $\sqrt{s} = 172$ GeV after the preselection and cut C1. The symbols are as defined in figure 1; signal events are of class C.
(b) The number of events versus the energy of the most energetic identified muon at $\sqrt{s} = 172$ GeV after the preselection and cuts C1-C3.

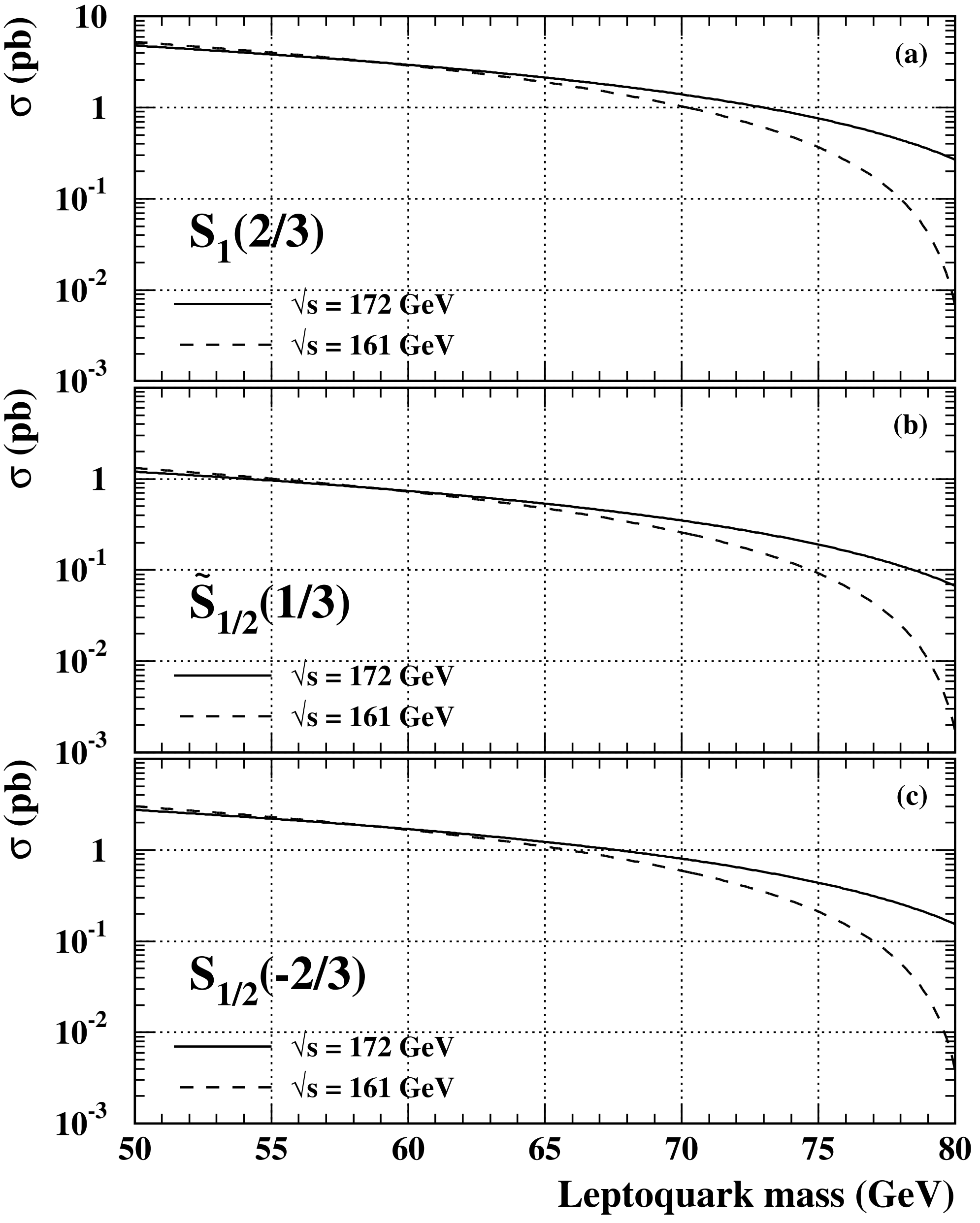

Figure 4:
The production cross sections at $\sqrt{s} = 161$ and 172 GeV of the leptoquark states $S_1(2/3)$ **(a)**, $\tilde{S}_{1/2}(1/3)$ **(b)** and $S_{1/2}(-2/3)$ **(c)**.

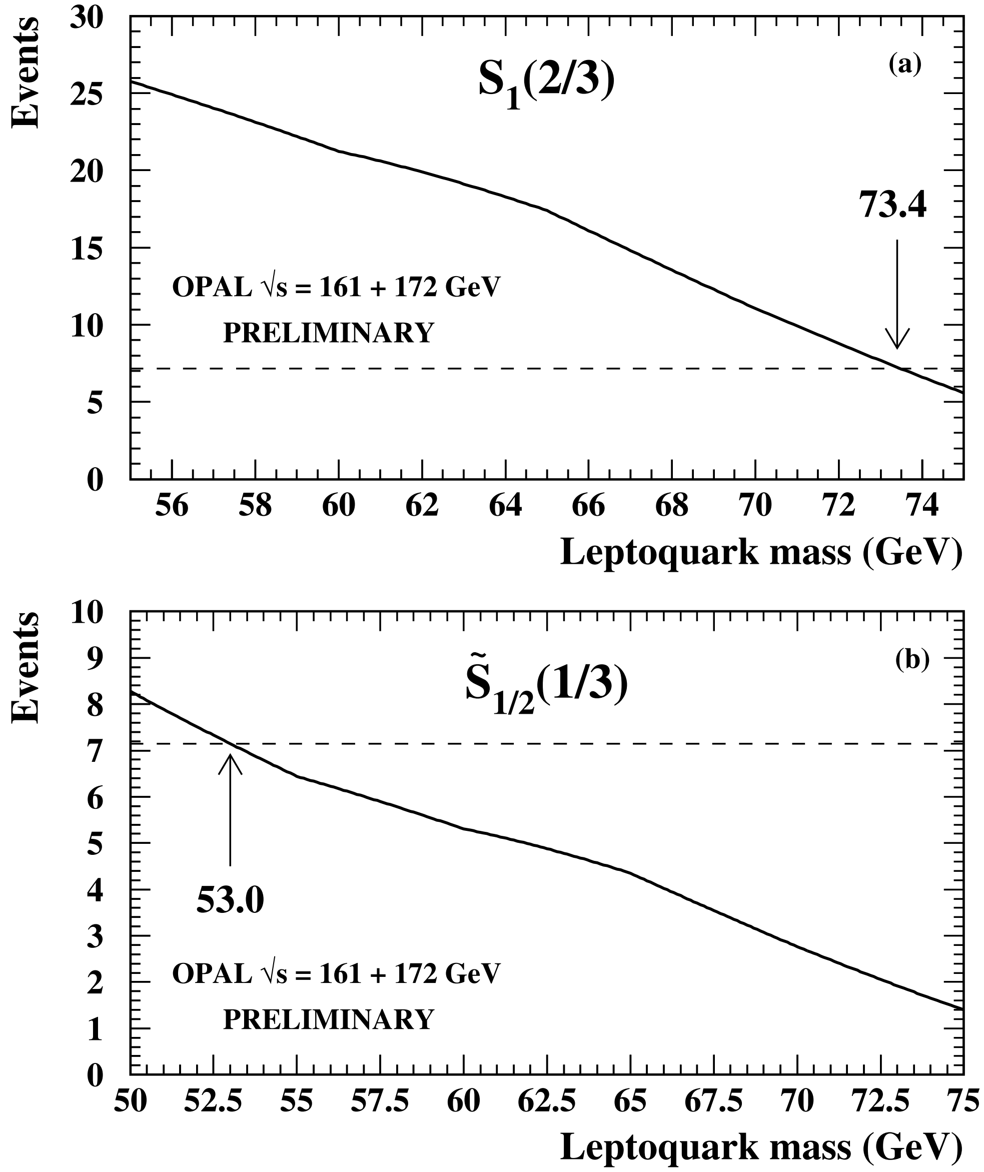

Figure 5:
(a) The expected number of events, computed by equation (1), as a function of the leptoquark mass M_{LQ}, for the state $S_1(2/3)$. The data at $\sqrt{s}$ = 161 and 172 GeV have been combined. The horizontal line is the 95% C.L. limit for three observed events.
(b) Same as (a) for the state $\tilde{S}_{1/2}(1/3)$.

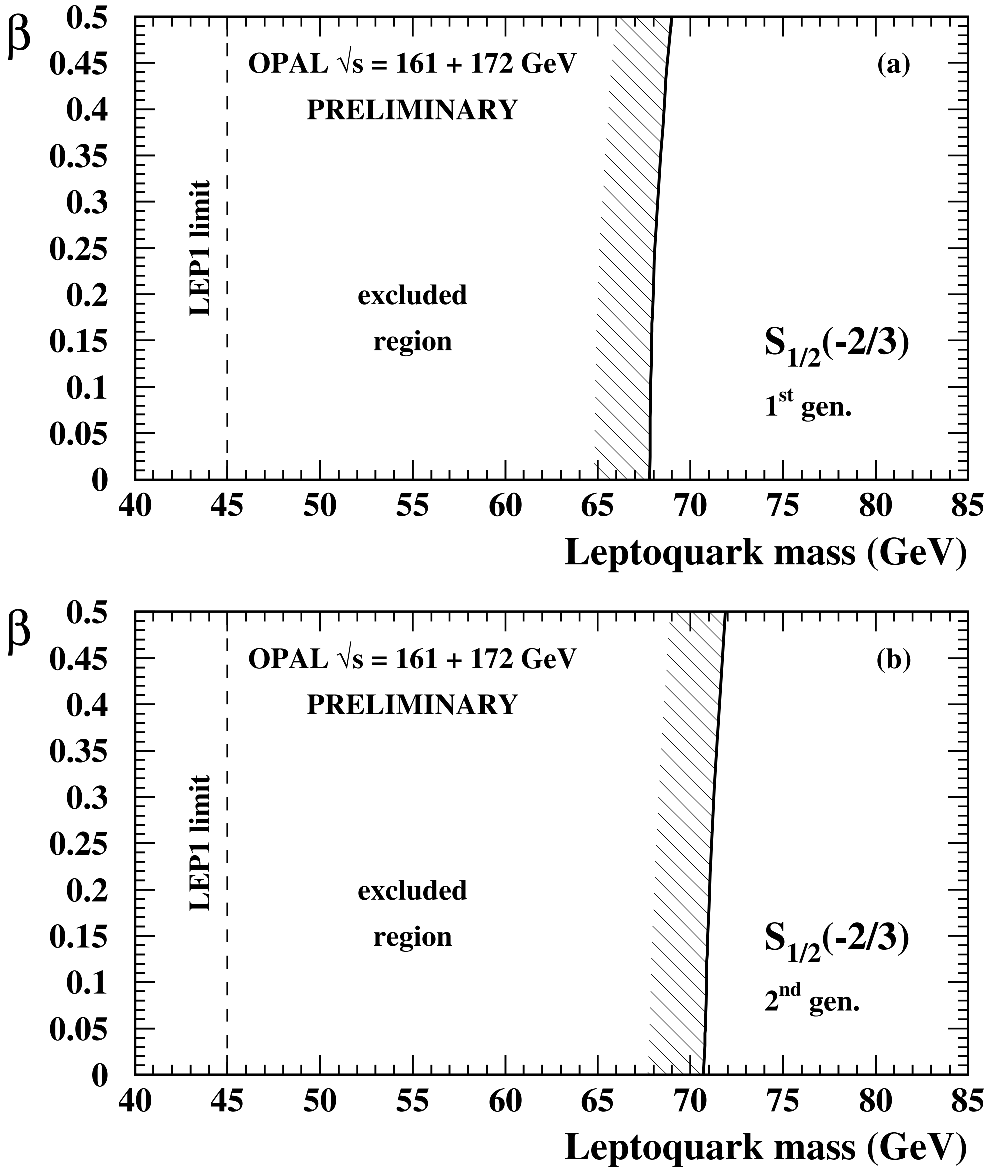

Figure 6:
(a) The 95% C.L. lower limits on M_{LQ}, as a function of β, for the state $S_{1/2}(-2/3)$, first generation. The data at $\sqrt{s} = 161$ and 172 GeV have been combined. The shaded area shows the excluded region.
(b) Same as (a), for the second generation.